International Conference on Applied Energy 2020
Dec. 1 - Dec. 10, 2020, Bangkok/Virtual
Paper ID: 9

Experimental investigation on performance, combustion and knock characteristics in a turbulent jet ignition (TJI) engine

Jianxiong Hua, Lei Zhou, Qiang Gao, Zhonghui Feng, Haiqiao Wei
State Key Laboratory of Engines, Tianjin University, Tianjin 300072, China

ABSTRACT

Turbulent jet ignition (TJI) shows great potentials of achieving lean combustion. In this work, a turbulent jet ignitor was designed and made, and the engine performance, combustion and knock characteristics were detailed studied in a single-cylinder engine. The results show that the lean burn limit is greatly extended through TJI combustion, and the indicated specific fuel consumption is apparently lower than that of spark ignition (SI) combustion under part load conditions. In TJI combustion, the flame jet leads to a fast burning rate at the beginning of the combustion; and with the fuel-air mixture becomes leaner, the burning rate gradually decreases while the spark timing needs to be advanced to keep appropriate combustion phase. In addition, pressure oscillations were both observed in TJI and SI combustions, in which the pressure oscillation of TJI is caused by the fast burning rate after the flame ejection, while that of SI is caused by the end-side auto-ignition. The spectrum analysis on knock frequency shows that the pressure oscillation modes of TJI and SI are different in the combustion chamber.

Keywords: turbulent jet ignition; lean burn; engine performance; knock

NONMENCLATURE

TJI	Turbulent Jet Ignition
SI	Spark Ignition
λ	Excessive Air Coefficient
°CA	Crank Angle Degree
IMEP	Indicated Mean Effective Pressure
ST	Spark Timing
HRR	Heat Release Rate
CoV	Coefficient of Variation
ISFC	Indicated Specific Fuel Consumption
MAPO	Maximum Amplitude of Pressure Oscillation
FFT	Fast Fourier Transform
CWT	Continuous Wavelet Transform

1. INTRODUCTION

Engine combustion with lean fuel-air mixture has potentials to achieve high thermal efficiency and low NOx emissions due to the high specific heat ratio and low heat loss to the cylinder wall. But when engine works with lean fuel-air mixture, poor ignition reliability and slow flame speed lead to severe incomplete combustion and poor combustion stability.

To solve this problem, turbulent jet ignition (TJI) with extra fuel supplement is one of the practical methods. With the application of a pre-chamber in an engine, a strong and hot product jet is generated when the flame passes through the jet holes [1]. Validi et al. [2] studied the detailed combustion process of TJI by large eddy simulation, and divided the whole combustion process into three stages, which are cold fuel jet phase, turbulent hot product jet phase and reverse fuel-air/product jet phase.

In engine studies, Attard [3, 4] realizes over 42% net indicated thermal efficiency and ultra-low NOx emissions (<10ppm) using TJI system, and they achieved extremely lean combustion with excessive air coefficient (λ) higher than 2.0. In addition, they also pointed out that TJI system with on extra fuel supplement is an effective way to extend knock limit [5]. Thelen et al. [6] investigated the effects of spark location on the performance of a TJI system, and found that locations furthest from the orifice provide better main chamber ignition and lead to faster burning rate in main chamber. Studies by Jamrozik et al. [7] and Bunce et al. [8] show that smaller orifice of the pre-chamber results in higher turbulence intensity in the main chamber, but too small orifice leads to choked flow jets and misfire in the main chamber.

Although many researches have been done focusing on TJI combustion, there are still many aspects needing to be studied, especially the detailed combustion features and knock characteristics. In this work, a turbulent jet ignitor with an auxiliary injection system is designed and made by house, and the experiments are conducted on a single-cylinder engine. The engine performance and combustion characteristics of TJI are detailed analyzed and compared with of SI combustion under the same engine loads. Furthermore, the knock characteristics of TJI and SI are comprehensive compared by statistical method, combustion analysis and spectrum analysis. This work provides valuable information and guidance to the application of TJI in real engines.

2. Experimental apparatus and procedures

2.1 Engine setup

The experiments were conducted on a single-cylinder, four-stroke Ricardo E6 engine with compression ratio of 10:1. The bore and stroke are 80mm and 100mm respectively, and more details can be found in Table 1. A house-made injection system, which controlled injection timing, injection pulse and rail pressure, was used in the experiments. Spark timings were adjusted by MoTeC 400.

The schematic of experimental apparatuses is shown in Fig. 1, where the testing equipment and combustion chamber arrangement are presented. The jet ignitor and fuel injector were side mounted on the cylinder head, and the injector utilized in the main-chamber was Siemens VDO piezoelectric injector. The engine speed was controlled by DZC-20 direct current dynamometer with uncertainty of ±0.2%. Fuel mass consumption was measured by a fuel consumption meter with a range of 5 kg/h and accuracy of ±0.2%. Temperatures of coolant and oil were monitored and adjusted by a SIEMENCE PID controller, and the temperature fluctuation of coolant was controlled within ±2 ^{o}C. Equivalence ratio was measured by a wideband lambda sensor with resolution of 0.001 and uncertainty of ±0.8%. The mass flow rate of intake air was measured by a Toceil LFE060 flow meter with uncertainty of ±1%. The in-cylinder pressure signal was collected by a Kistler 6118B pressure transducer, amplified by a Kistler 5018 charge amplifier and recorded by a combustion analyzer. With the synchronization signal of a photoelectric encoder, the resolution of the in-cylinder pressure signal was kept at 0.1 ^{o}CA.

Table 1 Specifications of experimental engine

Item	Description
Engine type	Single cylinder, four-stroke
Bore × stroke	80 mm × 100 mm
Sweep volume	0.5 L
Compression ratio	10:1
Valve mechanism	VVA, 2-valve
Injection system	Direct injection
TJI pre-chamber volume	3.6 ml
Jet hole of the pre-chamber	4mm, single hole

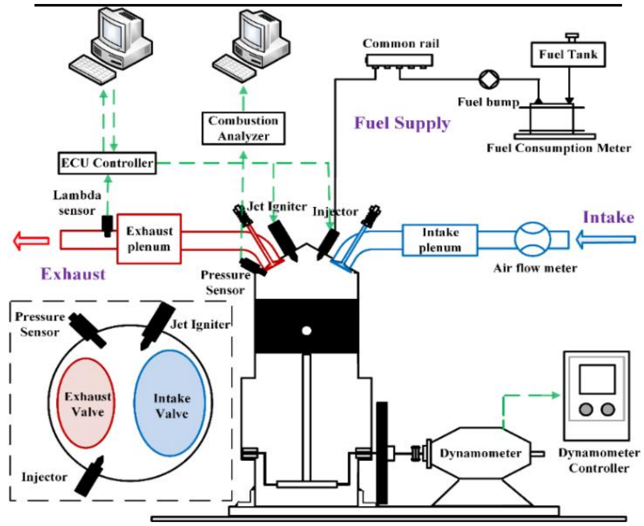

Fig. 1Experimental apparatuses

The structure of the pre-chamber with auxiliary fuel supplement is shown in Fig. 2, which comprises of a spark plug, a single-hole injector, and a pre-chamber housing. The single-hole injector was reformed from a commercial Bosch multi-hole injector by laser welding, and the spray direction is shown in Fig. 2. In addition, a coolant channel is designed in the housing of the pre-chamber to avoid damages of the single-hole injector by high combustion temperature. With the utilization of this pre-chamber, two injectors are needed; one is the normal injector to supply the demanded fuel in the main-chamber, and the other one is the single-hole injector with small flow coefficient to supply extra fuel in the pre-chamber.

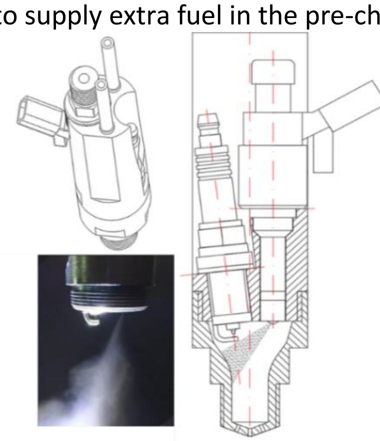

Fig. 2 Structure of the pre-chamber

2.2 Operation conditions

In experiments of the present work, the engine speed was kept constant at 1500 rpm, and the engine was naturally aspirated with an intake temperature of 20 °C±2 °C. The temperatures of coolant and lubricant oil were kept at 75 °C±3 °C and 85 °C±3 °C respectively. The fuel used throughout this work was Shell commercial gasoline with RON of 92. The injection pressure of both injectors in the main-chamber and the pre-chamber was set at 20 MPa in the experiments. The injection timing in the main-chamber was set at 300 °CA bTDC to generate homogeneous charge, and the injection timing of 180 °CA bTDC was set in the pre-chamber. Testing conditions of this work including TJI and SI combustions are listed in Table 2. The indicated mean effective pressure (IMEP) ranges from full load to low load by changing excessive air coefficients for TJI and changing throttle opening for SI. For each working condition, spark timings (STs) were scanned to cover maximum brake torque point.

Table 2 Test conditions

Combustion mode	IMEP (bar)	Throttle opening (%)	λ	ST (°CA bTDC)
TJI	3-9.5	100%	1.0-2.3	Scan to cover MBT point
SI	3-10	6%-100%	1.0	

To improve the accuracy and repeatability of the experiments, the data of 200 continuous cycles were recorded for every working condition. For analysis of the combustion process in the cylinder, the calculation of hear release rate (HRR) is necessary. A single-zone model based on the first law of thermodynamic[9, 10] is used in this work. The energy release from combustion is equal to the change in internal energy, the work that acts upon the piston, the heat transfer to the walls and the crevice loss, and the calculation of HRR is described as follows:

$$\frac{dQ_f}{d\varphi} = mc_v \frac{dT}{d\varphi} + \frac{pdV}{d\varphi} + \frac{A\bar{h}(T - Tw)}{d\varphi} + h_{cr}\frac{dm_{cr}}{d\varphi} \quad (1)$$

where Q_f is the energy release from combustion, φ is the crank angle degree, m and c_v are the instantaneous cylinder mass and mean specific heat at constant volume, T and T_w stand for in-cylinder temperature and wall temperature, p is the pressure in combustion chamber, A stands for combustion chamber surface area, $\bar{h}$ is heat transfer coefficient, which is calculated by Woschni formulation[9], m_{cr} and h_{cr} are defined as blow by mass from crevice region and the specific enthalpy. The crevice volume is assumed to be 2% of the clearance volume[11].

The coefficient of variations of indicated mean effective pressure (CoV_{IMEP}) is used to estimate the cycle-to-cycle variations of the experimental engine. The calculation is based on the in-cylinder pressure data of the 200 cycles. High cycle-to-cycle variation will affect the driving comfort, therefore the limit of CoV_{IMEP} is set at 5% in the present work.

3. Results and discussions

3.1 Engine performance of TJI combustion

In experiments of this work, both SI and TJI combustions were realized in the same engine. In SI combustion, the engine load was adjusted by varying throttle angle to keep the combustion at chemical stoichiometry. In TJI combustion, the engine load was adjusted by changing the excessive air coefficient (λ) while keeping the throttle widely opened. Fig. 3 shows the IMEP and ISFC of TJI combustion with different spark timings and λ. It is shown that λ has great effects on both IMEP and ISFC, that is, with λ increases from 1.0 to 2.2, the IMEP nearly decreases linearly, and the spark timings has little effects on IMEP. But for ISFC, it firstly decreases and then increases with λ changing from 1.0 to 2.2, and the lowest ISFC is acquired between λ of 1.4-1.6. Lean combustion reduces the heat dissipation and enhances the specific heat ratio of the gas, which improves the fuel economy, but too lean combustion increases the incomplete of combustion, leading to obvious increases of ISFC.

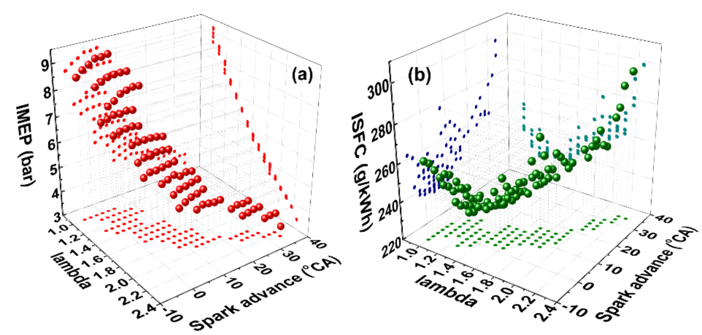

Fig. 3 IMEP and ISFC of TJI combustion with different spark timings and lambdas

Fig. 4 compares ISFC and CoV_{IMEP} of SI and TJI combustion. The result shows that the TJI combustion has apparently lower ISFC under part load conditions with IMEP between 3.5-8.5 bar. As for the stability, both SI and TJI have very low cyclic variations with IMEP higher than 4 bar. But when IMEP is lower than 4 bar, the CoV_{IMEP} dramatically increases due to the excessively lean fuel-air ratio (λ higher than 2.0). Considering the engine load of TJI is controlled by adjusting excessive air coefficient, lower load corresponds to leaner fuel, which is the main reason of deterioration of combustion stability under low engine loads when applying TJI combustion.

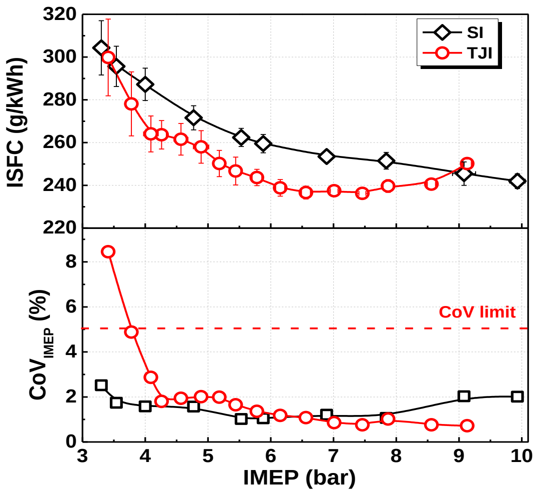

Fig. 4 Comparison between SI and TJI on ISFC and CoV$_{IMEP}$

3.2 Combustion characteristics of TJI combustion

Due to the existence of the pre-chamber and the jet hole, combustion characteristics of TJI and SI vary a lot. Fig. 5 shows the in-cylinder pressures and HRRs of TJI and SI combustion at excessive air coefficient of 1.0. In this figure, the TJI and SI condition have almost the same IMEP and CA50. It can be seen that in SI combustion, the HRR gradually rises to reach the peak, and then gradually decreases. For TJI combustion, the flame firstly propagates in the pre-chamber, leading to a minor increase of the HRR. Then, after the flame ejects into the main-chamber, a sudden increase of HRR occurs, leading to a fast combustion process. And next, the burning rate decreases as the flame propagates to burn off the remainder of the fuel. The combustion duration of TJI is definitely shorter than that of SI with the same combustion phase CA50.

Fig. 6 shows the in-cylinder pressures and HRRs of TJI with various λ. For each λ, spark timing was swept to find the maximum brake torque point. It is seen in Fig. 6 that with fuel-air mixture becomes leaner, more advanced spark timing or start of combustion is needed to keep proper combustion phase. In addition, leaner fuel clearly leads to a reduction of HRR peak, which is due to the reduction of energy density in combustion chamber and the decline of the mixture reactivity.

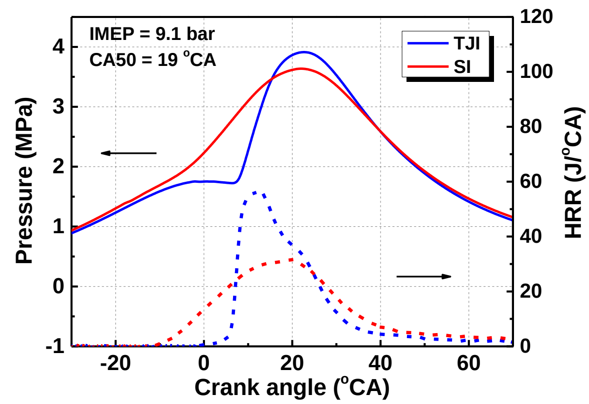

Fig. 5 Combustion comparison between TJI and SI at excessive air coefficient of 1.0

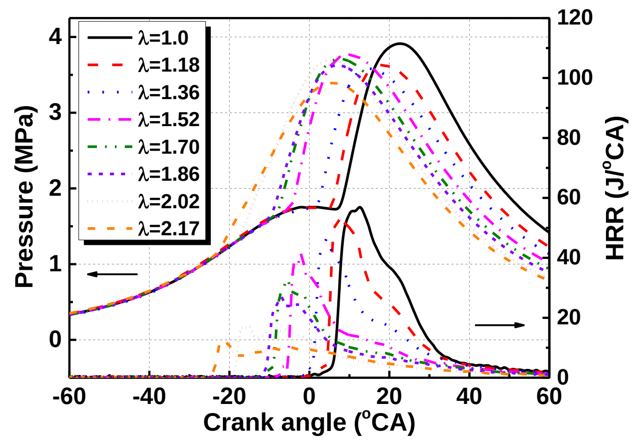

Fig. 6 In-cylinder pressures and HRRs of TJI with various excessive air coefficient

3.4 Knock characteristics of TJI combustion

In the discussions above, TJI combustion generates strong flame jets in the main chamber and causes a very rapid increase on HRR. As is known to us, the local violent heat release can generate large pressure gradients and even pressure waves, which is the main feature of knocking combustion. Therefore, in this section, the pressure oscillations of TJI combustion are detailed analyzed. Fig. 7 shows the maximum amplitude of pressure oscillation (MAPO) distributions of TJI and SI combustion modes against spark timings. The conditions have nearly the same engine load and IMEP. It is seen that the MAPO mean value and the median TJI combustion approximately linearly increase, and almost no abnormal cycle with extremely high MAPO exists. However, in SI combustion, the MAPO distributions of knock-free conditions are almost the same, but when knock happens, a sudden increase of MAPO mean valve is observed with the existing of some abnormal combustion cycles, which have extremely high knock intensity.

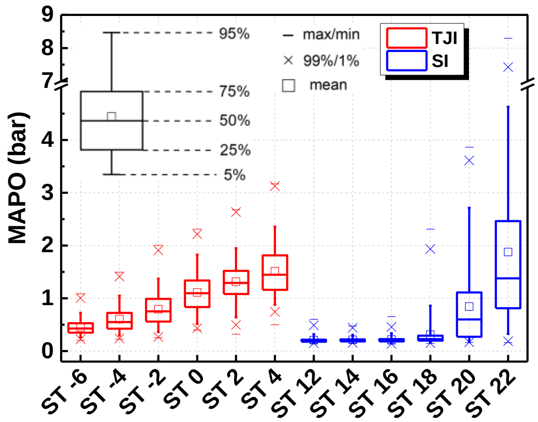

Fig. 7 MAPO distributions of TJI and SI combustion modes against spark timings

Furtherly, to investigate the detailed combustion process of TJI with pressure oscillations, several representative combustion cycles, including TJI knock, TJI normal, SI knock and SI normal cycles, are plotted in Fig. 8. The cycles of TJI knock and SI knock have similar MAPO, which is approximately 2.0 bar. In the figure, it is clear that the pressure oscillation starts after the rapid increase of HRR in both SI and TJI knock combustions, but the causes of the rapid increases on HRR are different. In TJI combustion, the pressure oscillation is caused by the fast burning rate when the flame jets eject from the pre-chamber into the main chamber; while the pressure oscillation in SI knock is caused by a sudden heat release process of an end-side auto-ignition point. In addition, compared with TJI knock and TJI normal cycles, it can be seen that regardless of the knock intensity, the rapid increase on HRR always exists; but in SI normal cycles, the sudden increase of HRR caused by end-side auto-ignition is not happened, which means the phenomenon of pressure oscillation of SI combustion has stronger randomness than that of TJI combustion.

Next, frequency analysis is conducted using the two knocking cycles of TJI and SI plotted in Fig. 8. In many literatures[12, 13], frequency analysis is performed by Fast Fourier Transform (FFT) algorithm, which presents a result of amplitude against frequency. But the FFT result presents no information against time, therefore, continuous wavelet transform (CWT) algorithm is implemented in the present work to derive information that includes a signal of frequency and a signal of time. The results that include both frequency and time information of SI knock and TJI knock are provided in Fig. 9 (a) and (b). It is observed that at beginning of the pressure oscillation in TJI knock, the frequency is relatively low, and as time passes the frequency rises to approximately 7.5 kHz. The reason is that when pressure waves were generated by flame jet in main-chamber, the ambient temperature is low, which leads to low pressure wave speed and low frequency of pressure oscillations. And as combustion carries on, the temperature gradually increases, leading to higher pressure wave speed, which results in the rising of pressure oscillation frequency. Compared knock frequencies of TJI and SI, only two knock frequencies are observed in TJI knock, while three frequencies are observed in SI knock, which indicates different pressure oscillations modes in the combustion chamber.

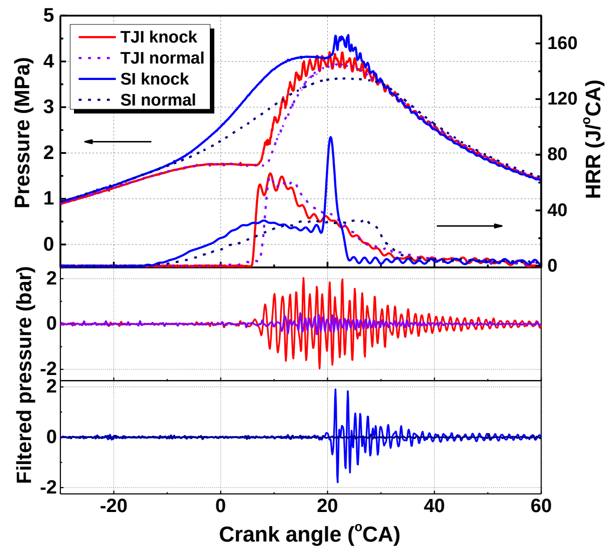

Fig. 8 In-cylinder pressures, HRRs and pressure oscillations of TJI and SI combustion modes

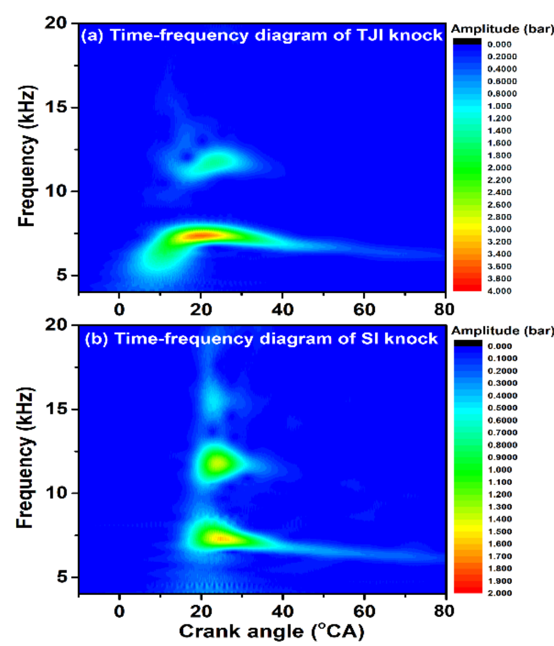

Fig. 9 Time-frequency diagram of SI knock and JI knock

4. Conclusions

A turbulent jet ignitor has been designed and made in this work, and tests on engine performance, combustion and knock characteristics have been conducted. The key conclusions are as follows:

1. TJI combustion has great potential for achieving lean combustion due to the existence of the pre-chamber with extra fuel supplement. In lean burn situations, the lowest ISFC of TJI is obtained with λ between 1.4-1.6. Compared with SI combustion, the ISFC of TJI combustion is apparently lower than that of SI combustion, especially under part load conditions.
2. In TJI combustion, a rapid increase on HRR is observed at the beginning of the combustion process due to the fast burning rate caused by the strong flame jets. In lean burn conditions, the peak of HRR gradually decreases due to the reduction of energy density and mixture reactivity. Therefore, spark timings should be advanced to maintain optimal combustion phase.
3. Pressure oscillations can be observed in both TJI and SI combustions, in which the pressure oscillation of TJI is caused by the fast burning rate after the flame ejection, while that of SI is caused by the end-side auto-ignition. Therefore, some abnormal cycles with extremely high knock intensity can be observed in SI knock, while almost no abnormal cycles can be found in TJI knock. In addition, the spectrum analysis on knock frequency by using CWT algorithm shows that the pressure oscillation modes of TJI and SI are different in combustion chamber.

ACKNOWLEDGEMENT

The work was supported by the National Natural Science Foundation of China (51706152, 51825603), the National Key Research and Development Program of China (2017YFB0103400), and the National Science Fund for Distinguished Young Scholars (51825603).

REFERENCE

[1] Biswas S, Tanvir S, Wang H, Qiao L. On ignition mechanisms of premixed CH 4 /air and H 2 /air using a hot turbulent jet generated by pre-chamber combustion. Appl Therm Eng. 2016;106:925-37.
[2] Validi A, Schock H, Jaberi F. Turbulent jet ignition assisted combustion in a rapid compression machine. Combustion and Flame. 2017;186:65-82.
[3] Attard WP, Parsons P. A Normally Aspirated Spark Initiated Combustion System Capable of High Load, High Efficiency and Near Zero NOx Emissions in a Modern Vehicle Powertrain. SAE International; 2010.
[4] Attard WP, Fraser N, Parsons P, Toulson E. A Turbulent Jet Ignition Pre-Chamber Combustion System for Large Fuel Economy Improvements in a Modern Vehicle Powertrain. SAE International; 2010.
[5] Attard WP, Blaxill H, Anderson EK, Litke P. Knock Limit Extension with a Gasoline Fueled Pre-Chamber Jet Igniter in a Modern Vehicle Powertrain. SAE International; 2012.
[6] Thelen BC, Toulson E. A Computational Study of the Effects of Spark Location on the Performance of a Turbulent Jet Ignition System. SAE International; 2016.
[7] Jamrozik A, Tutak W, Kociszewski A, Sosnowski M. Numerical simulation of two-stage combustion in SI engine with prechamber. Applied Mathematical Modelling. 2013;37:2961-82.
[8] Bunce M, Blaxill H, Kulatilaka W, Jiang N. The Effects of Turbulent Jet Characteristics on Engine Performance Using a Pre-Chamber Combustor. SAE International; 2014.
[9] Heywood JB. Internal Combustion Engine Fundamentals: McGraw-Hill; 1988.
[10] Rakopoulos CD, Antonopoulos KA, Rakopoulos DC. Experimental heat release analysis and emissions of a HSDI diesel engine fueled with ethanol–diesel fuel blends. Energy. 2007;32:1791-808.
[11] Cooney C, Worm J, Naber J. The calculation of mass fraction burn of ethanol-gasoline blended fuels using single and two-zone models. SAE Technical Paper 2008-01-0320; 2008.
[12] Galloni E, Fontana G, Staccone S. Numerical and experimental characterization of knock occurrence in a turbo-charged spark-ignition engine. Energy Conversion and Management. 2014;85:417-24.
[13] Naruke M, Morie K, Sakaida S, Tanaka K, Konno M. Effects of hydrogen addition on engine performance in a spark ignition engine with a high compression ratio under lean burn conditions. International Journal of Hydrogen Energy. 2019;44:15565-74.